Journal of Ovonic Research Vol. 3, No. 1, February 2007, p. 1 - 13

CALORIMETRIC ANALYSIS OF Ag DOPED AMORPHOUS Se-Sb CHALCOGENIDE GLASSES

K. S. Bindra, Nikhil Suri, M. S. Kamboj[a], R. Thangaraj[*]

Semiconductors Laboratory, Department of Applied Physics, Guru Nanak Dev University, Amritsar-143005, Punjab, India
[a] Department of Elelctrical Computer Engineering, Ryerson University, 350 Victoria Street Toronto, Ontario M5B 2K3 Canada

Calorimetric analysis of bulk amorphous $Se_{80-x}Sb_{20}Ag_x$ ($8 \leq x \leq 14$) glasses has been carried out using Differential Scanning Calorimetry at different heating rates (5-20 K/min). It is found that the glass transition temperature T_g and the crystallization temperature T_c increase with increase in Ag content in Se-Sb system. The apparent activation energy for glass transition and the activation energy for crystallization have been determined using different empirical approaches. The glass-forming ability of amorphous $Se_{80-x}Sb_{20}Ag_x$ increases with Ag content.

(Received January 25, 2007, accepted January 30, 2007)

Keywords: Amorphous semiconductors, Chalcogenide glasses, Glass transition, Thermal stability

1. Introduction

Recently, great attention has been given to chalcogenide glasses mainly due to their wide range of application in solid-state devices both in scientific and technological fields. Optical data storage based on laser induced amorphous-to-crystalline phase transformation of chalcogenide glasses is an area with on-going research activity. Since the advent of optical memory storage, a-Se has become a material of considerable commercial importance in optical memory applications [1-6]. As the uses of Se have grown, the attempts have been made to improve certain of its properties by alloying with other elements.

The structure of a-Se and the effect of alloying Sb instead of As have been studied by various workers due to the toxic nature of the latter limiting the practical applications. The addition of Sb in a-Se has pronounced effect on its structural, optical, electronic and thermal properties [7-9]. Due to these advantages, Se-Sb alloys can be used as recording layer materials in optical phase change recording technique. Ag-doped chalcogenide glasses have become attractive materials for fundamental research of their structure, properties and preparation [10-14]. They have many current and potential applications in optics and optoelectronics such as photo doping, optical imaging, photo lithography and phase change optical recording [15-21].

The electrical, optical and structural properties of Ag doped chalcogenide glasses have been studied by various workers [10-21] but there are only few studies reported on crystallization in these materials [22-25]. The crystallization kinetics in chalcogenide glasses can be studied using isothermal and non-isothermal methods. The present work reports on the crystallization kinetics of amorphous $Se_{80-x}Sb_{20}Ag_x$ ($8 \leq x \leq 14$) using non-isothermal method.

---

[*] Corresponding author: rthangaraj@rediffmail.com

2. Experimental details

Bulk samples of $Se_{80-x}Sb_{20}Ag_x$ ($8 \leq x \leq 14$) for all composition were prepared by melt quenching technique. High-purity (99.99%) elements were weighed according to their atomic percentage, and were sealed in a quartz ampoule (length ~10cm and internal diameter ~6mm), in a vacuum of $\sim 10^{-4}$ mbar. The sealed ampoule was kept in a vertical furnace where the temperature was raised to 1273 K at a rate of 4-5 K/min. The ampoule was inverted at a regular interval (~1 h) for 48 h at the maximum temperature to make sure the homogenous mixing of the constituents, before quenching into an ice bath. The material was separated from the quartz ampoule by dissolving the ampoule into a solution of HF + H_2O_2 for approximately 48h. The amorphous nature of the sample was confirmed by absence of sharp peaks in X-ray diffractograms. DSC runs were carried out using Mettler Toledo Star^e instrument. The DSC equipment was calibrated with standard materials prior to start of the experiment. All the DSC scans were performed under N_2 atmosphere. About 25 mg of the powdered sample was placed in the aluminum pans for the studies. DSC thermograms for all the compositions were taken at different heating rates [5,10,15 and 20 K/min]. The glass transition temperature (T_g) was taken as the temperature corresponding to the intersection of the two linear portions adjoining the transition elbow of the first endothermic peak in the DSC plots. The T_c was taken as the temperature corresponding to the onset of crystallization, where the crystallization has just started. The fraction X crystallized at any temperature T is calculated as $X = A_T/A$, where A is the total area of the exotherm between T_c and the temperature at which the crystallization is completed, A_T is the area of the exothermal between T_c and T [34].

3. Results and discussion

Typical DSC thermograms at the heating rate of 15 K/min for $Se_{80-x}Sb_{20}Ag_x$ (x=8, 10, 12, 14) are shown in Fig. 1. All the thermograms show glass transition, crystallization and melting. There is also an endothermic peak after the glass transition which may be due the relaxation of the metastable glass. Fig. 2 shows the DSC thermograms of $Se_{72}Sb_{20}Ag_8$ glass at four different heating rates. The characteristic phenomena (glass transition and crystallization) are evident in all the DSC thermograms in the temperature range of investigation. One can see from Fig. 2. that T_g and T_c shift towards higher temperature with increase in heating rate whereas there is no variation in T_m with increase in the heating rate. The system shows similar behavior for all the values of x.

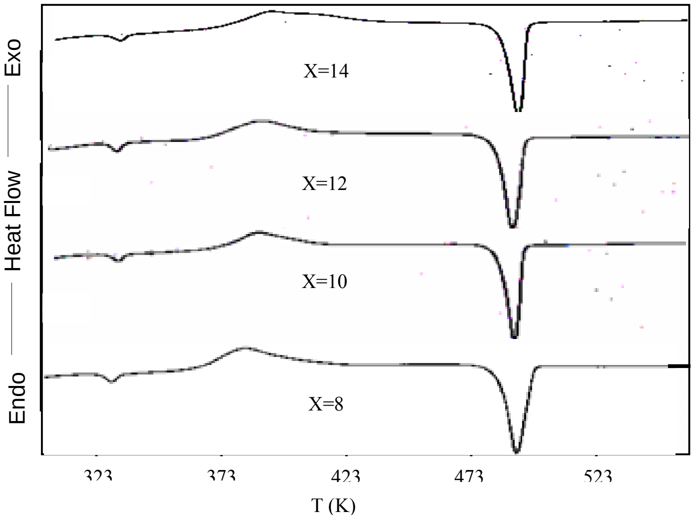

Fig. 1. DSC thermogram for $Se_{80-x}Sb_{20}Ag_x$ ($8 \leq x \leq 14$) at heating rate of 15 K/min.

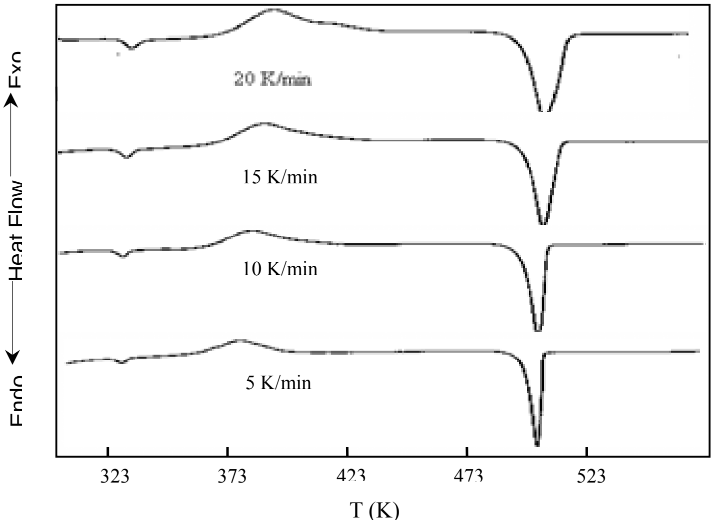

Fig. 2. DSC thermogram for $Se_{72}Sb_{20}Ag_8$ at four different heating rates.

It has been observed that T_g increases with increase of Ag concentration and varies linearly with the heating rate as shown in Fig. 3.

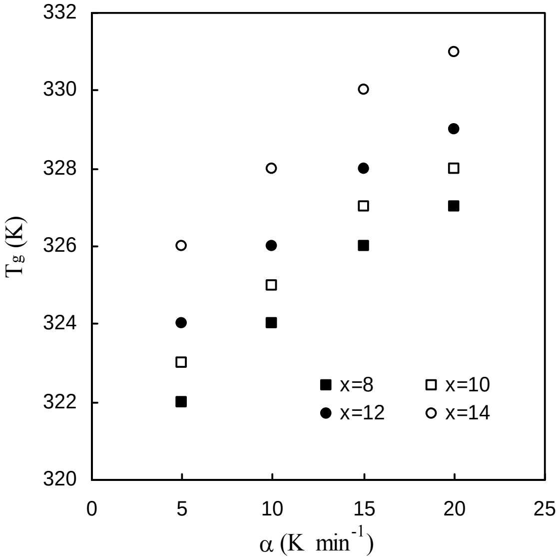

Fig. 3. Variation of glass transition temperature with heating rates for $Se_{80-x}Sb_{20}Ag_x$ ($8 \le x \le 14$).

The values of T_c of each alloy are found to be much higher than the room temperature. This is an important advantage of these alloys, which is essential to prevent self-transition of recording materials between the two phases; amorphous and crystalline phase at room temperature. The dependence of T_g on the heating rate has been studied using three different formulations. The first one corresponds to the empirical relation of the form

$$T_g = \mathrm{A} + \mathrm{B}\ln(\alpha) \tag{1}$$

where A and B are constants that depend on the glass composition and α is the heating rate (K/min) employed in DSC runs [26]. Fig. 4 shows the validity of this equation for $Se_{72}Sb_{20}Ag_8$. The value of B is calculated from the slope of T_g vs. ln (α) plots. It has been suggested that B depends on the cooling rate employed in the preparation and is the indicator of the response of configurational changes within the glass transition region to the heating rate [26]. The values of A and B for all compositions are listed in Table 2.

The variation of glass transition temperature with heating rate is shown in Fig.3 and it is found that T_g varies linearly with the heating rate and this variation may be described by the empirical formula [27]

$$T_g = T_o' + S\alpha \tag{2}$$

where T_o' is the glass transition temperature at zero heating rate, normally depicted as ideal glass transition temperature. The values of T_o' and S for all compositions are listed in Table 1.

Table. 1. The thermal parameters of the investigated samples as a function of Ag content.

Alloy	T_g (K)				T_o'	S	E_t(kJmol^{-1})
	Heating Rate (K min^{-1})				(K)		
	5	10	15	20			
$Se_{72}Sb_{20}Ag_8$	322	323	324	326	320±0.5	0.34	238±0.5
$Se_{70}Sb_{20}Ag_{10}$	324	325	326	328	321±0.5	0.34	240±0.8
$Se_{68}Sb_{20}Ag_{12}$	326	327	328	330	322±0.5	0.34	242±0.7
$Se_{66}Sb_{20}Ag_{14}$	327	328	329	331	324±0.5	0.34	245±0.4

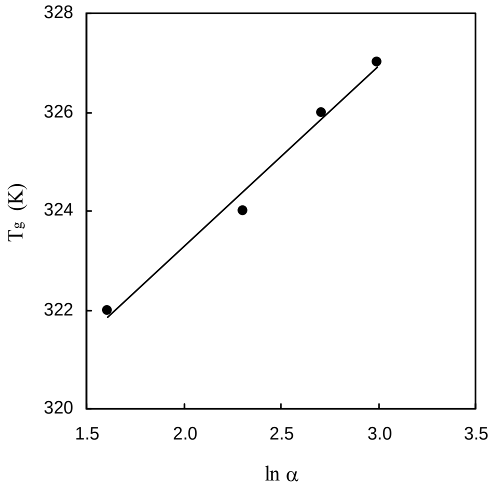

Fig. 4. Variation of T_g with ln α for $Se_{72}Sb_{20}Ag_8$

The third approach to the study of dependence of T_g on the heating rate is the Kissinger [28] formulation for the evaluation of the apparent activation energy of glass transition, E_t. In spite of the fact that the Kissinger equation is basically for the determination of the activation energy for crystallization process, it has been shown that the same equation can be used for evaluation of E_t [29-32], and may be written as

$$\ln\frac{T_g^2}{\alpha} = \frac{\mathrm{E_t}}{\mathrm{R}T_g} + \mathrm{const.} \qquad (3)$$

where R is the gas constant.

Fig. 5. shows the plot of ln (T_g^2/α) as a function of 1000/ T_g for $Se_{72}Sb_{20}Ag_8$. The slope of the plot gives the apparent activation energy, E_t. The values of E_t for all the compositions are given in Table 1. The glass activation energy is the amount of energy that is absorbed by a group of atoms in the glassy region so that a jump from one metastable state to another metastable state is possible [33].

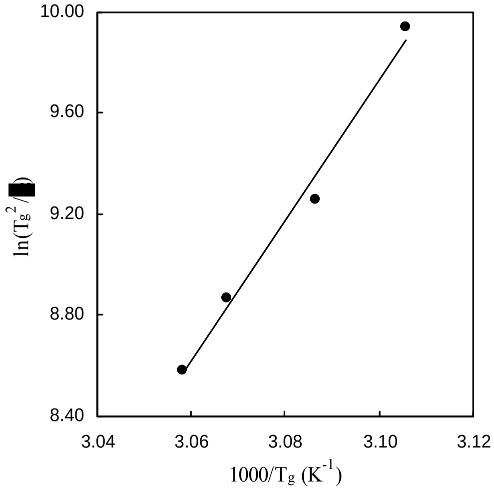

Fig. 5. A plot of $\ln(T_g^2/\alpha)$ vs. $1000/T_g$ for $Se_{72}Sb_{20}Ag_8$

From technological application points of view, the glass should be thermally stable with temperature and time during use. The kinetic resistance to crystallization is higher for larger difference between T_c and T_g. The difference T_c-T_g, which is an indication of thermal stability of glasses [34], increases as Ag contents increase in these glasses as shown in Fig. 6. for all heating rates. It shows that it is easier to prepare glasses with higher concentration of Ag as compared to lower concentration of Ag. It has been reported that enthalpy ΔH_c released during crystallization process is associated with stability of glasses i.e. glasses with lowest value of T_c-Tg will have maximum value of ΔHc.

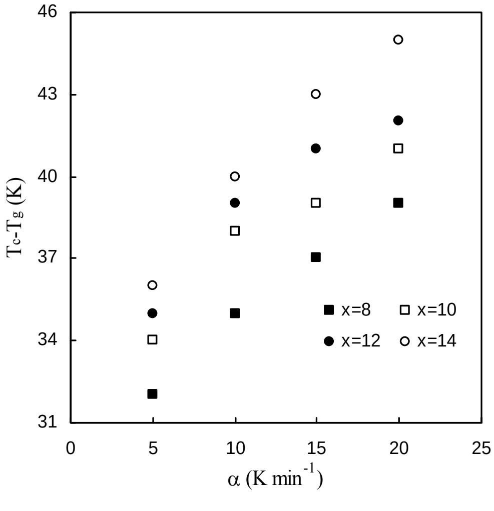

Fig. 6. A plot of T_c-T_g vs. heating rate for $Se_{80-x}Sb_{20}Ag_x$ ($8 \leq x \leq 14$).

The experimental determination of enthalpy-released ΔH_c during crystallization process has been made by measuring the area under exothermic peak and converted it into units of milli calorie.

$$\frac{\Delta H_c}{K'} = \frac{A_c}{M} \tag{4}$$

where K' is the instrumentation constant. A_c is the area under the crystallization peak and M is the mass of the sample.

The value of $\Delta H_c/K'$ at all heating rates is plotted as a function of Ag content in Fig. 7. It is seen that $\Delta H_c/K'$ keeps on decreasing with Ag content. It can be noted that the difference of T_c-T_g increases with x where as the enthalpy released decreases with x. This shows with the increase of Ag contents in Se-Sb matrix increases thermal stability.

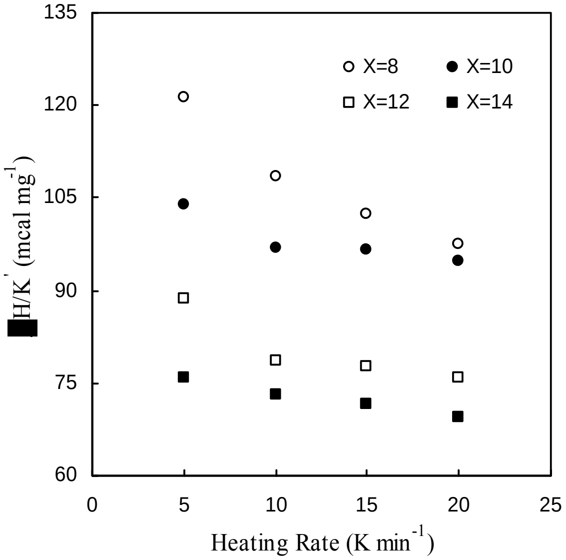

Fig. 7. A plot of enthalpy released vs. heating rate for $Se_{80-x}Sb_{20}Ag_x$ ($8 \le x \le 14$)

The kinetics of crystallization as a function of composition has been studied. The most successful and applicable theoretical model for crystallization studies is the one suggested by Johnson-Mehl-Avrami (JMA) [35-38]. According to this model, the fraction, X, of precursor that has been transformed into product phase is given by

$$X = 1 - \exp\left(-K_a t^n\right) \tag{5}$$

Where, n is the Avrami exponent and reflects the details of crystal growth, K_a is the effective overall reaction rate, which actually reflects the rate of crystallization [39] and usually assigned Arrhenian temperature dependence,

$$K_a = K_o \exp\left(-\frac{E}{RT}\right) \tag{6}$$

Here K_o, the frequency factor, indicates the number of attempts to overcome the energy barrier, E is the activation energy. In heterogeneous reaction, such as crystallization, activation energy is superimposed on more than one energy [40], basically growth and nucleation activation energies.

The JMA equation has been developed to study the kinetics of phase transformations involving nucleation and growth processes. However, if a transformation consisting of nucleation and growth occurs non-isothermally, it can still be described by the JMA equation if the following conditions are satisfied [41,42]. Firstly, all nucleation should occur at early stages of the process, secondly, the nucleation is random and, finally, if the growth rate depends on instantaneous temperature and not on time. In our case the transformation will have identical form at all temperatures. According to Cahn [43] for isokinetic reaction, the instantaneous rate of transformation is a unique function of the extent of transformation, X, and absolute temperature T, and is entirely independent of prior thermal history.

The temperature dependence associated with the JMA transformation assumed that in glass forming system K_a could demonstrate a single Arrhenian behavior given by Eq. (vi). since it is extremely doubtful whether both the nucleation and crystal growth rate [41] will have the same temperature dependence during observable non-isothermal crystallization process. This restricts the temperature range of possible experiments to temperature regimes where the growth rate is dominated by molecular mobility in the liquid phase (i.e. K_a depends only on the growth rate and not on the nucleation rate). Specially, this temperature regime refers to the low temperature side of the peaked growth rate curve [44]. Thus in order to experimentally obtain the simplified temperature dependence for K_a given by Eq. (vi). in glass forming liquid, scans from low to high temperatures must be used which allow the melt to fully crystallize at temperatures which are dominated by low temperature growth behavior.

Extending the use of JMA equation to interpret the dynamic heating (non-isothermal) data is controversial since the analysis requires time differentiation of JMA equation with the implicit assumption that the process parameters are independent of time [45,46]. Following White and Crane [47] the non-isothermal equation obtained from JMA, equation is given by

$$\ln\frac{\alpha}{T_p} = \text{const.} - \frac{\mathrm{E}}{\mathrm{nR}T_p} \tag{7}$$

where, T_p is the temperature at which the crystallization attains the maximum value and considered to be the peak temperature of the exothermic reaction in DSC curves.

The non-isothermal activation E/n has been interpreted as the activation energy for the rate-limiting step for growth at the interface during crystallization as inter-atomic diffusion [41]. Fig. 8. shows the plot of ln (α/T_p) as a function of $1000/T_p$ for $Se_{72}Sb_{20}Ag_8$ glass. The values of E/n for all the glasses are listed in Table 2.

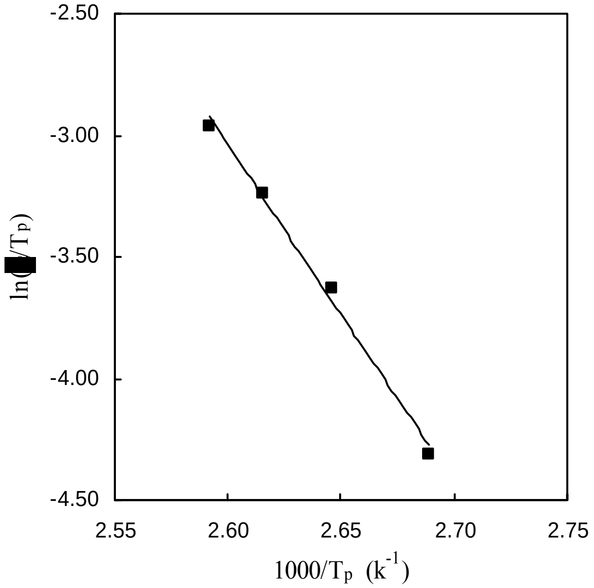

Fig. 8. The plot of ln (α/T_p) as a function of $1000/T_p$ for $Se_{72}Sb_{20}Ag_8$ glass.

Table. 2. The values of A and B along with E_c for $Se_{80-x}Sb_{20}Ag_x$ (8≤x≤14) glassy system.

Alloy	A	B	E_c (kJ $mole^{-1}$)			
	(K)	(K)	JMA	Matusita	Kissinger	Ozawa
$Se_{72}Sb_{20}Ag_8$	315±1	3.66±0.4	117±0.8	116±1.0	114±4.5	131±1.7
$Se_{70}Sb_{20}Ag_{10}$	316±1	3.50±0.4	114±0.6	113±1.0	111±3.4	133±1.5
$Se_{68}Sb_{20}Ag_{12}$	317±1	3.34±0.3	113±0.8	111±0.8	109±2.0	130±1.2
$Se_{66}Sb_{20}Ag_{14}$	319±1	3.22±0.4	102±0.9	110±1.1	98±1.5	108±1.5

For the determination of activation energy of crystallization, Matusita et al. [48] have suggested an equation, which is applicable for non-isothermal crystallization and is given by

$$\ln[-\ln(1-X)] = -n\ln(\alpha) - 1.052\frac{mE_c}{RT} + \text{const.} \tag{8}$$

where, X, is the volume of fraction crystallized at any temperature, n and m are constants related to crystallization mechanism. For as-quenched glasses containing no pre-existing nuclei, n = m+1, whereas for glass containing a sufficiently large number of nuclei n = m [48]. The value of n and m can be obtained by plotting ln [-ln (1-X)] as a function of ln (α) at a specific temperature. Fig. 9. shows the plot ln [-ln (1-X)] vs. ln (α) for $Se_{72}Sb_{20}Ag_8$ glass at three different temperatures. A small variation in the values of n is observed. The average value of n, as evaluated from the slope of plots at three temperatures, comes to 2.62 (~3). Since ours are quenched samples, the value of m is one less than n, therefore, the value of m is 2 which may indicates that the bulk nucleation with two-dimensional growth occurs in these glasses.

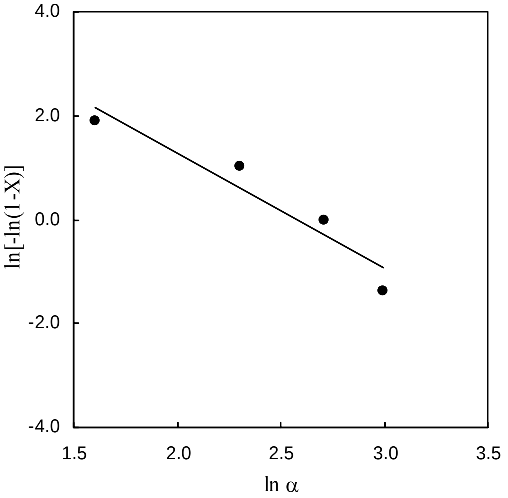

Fig. 9. A plot of ln[-ln (1-X)] as a function of ln α for $Se_{72}Sb_{20}Ag_8$

In order to evaluate the activation energy from Matusita equation, the slope of plot of ln [-ln(1-X)] vs. 1000/T at different heating rates as shown in Fig. 10. for $Se_{72}Sb_{20}Ag_8$. It is observed that the plots are linear over a wide temperature range but show a break at higher temperatures, which is attributed to the saturation of nucleation sites in the final stages of crystallization [49,50] or to restriction of the crystal growth in the small size of particles [51]. The initial region extending over large range is used for the determination of slopes. The activation energies as calculated from slope of these plots is listed, in Table 2.

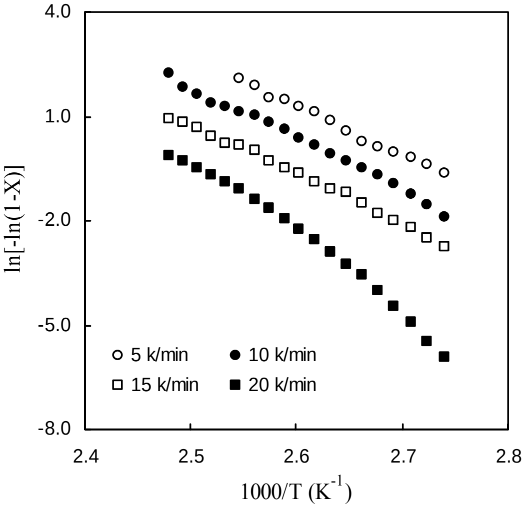

Fig. 10. A plot of ln[-ln (1-X)] vs. 1000/T at different heating rates for $Se_{72}Sb_{20}Ag_8$

The activation energy of crystallization E_c has also been evaluated using peak shift method of Kissinger [28] this method involves the use of the equation

$$\ln\frac{\alpha}{T_p^2} = -\frac{\mathrm{E_c}}{\mathrm{R}T_p} + \mathrm{const} \tag{9}$$

where T_p is the temperature of crystallization peak. The activation energies for all the composition have been determined from the slope of the plot of ln (α/T_p^2) vs. $1000/T_p$ as shown in Fig. 11. The values of E_c, for all the composition are given in Table 2.

Ozawa [52] suggested another method for evaluation of the crystallization activation energy from the variation of the onset crystallization temperature, T_c with the heating rate. This method involves the use of following equation,

$$\ln\alpha = -\frac{\mathrm{E_c}}{\mathrm{R}T_c} + \mathrm{const.} \tag{10}$$

Fig. 12. show the plot of ln (α) as a function $1000/T_c$ for $Se_{72}Sb_{20}Ag_8$ glass, the slope of which gives the activation energy E_c. The values of E_c for all the composition are given in Table2.

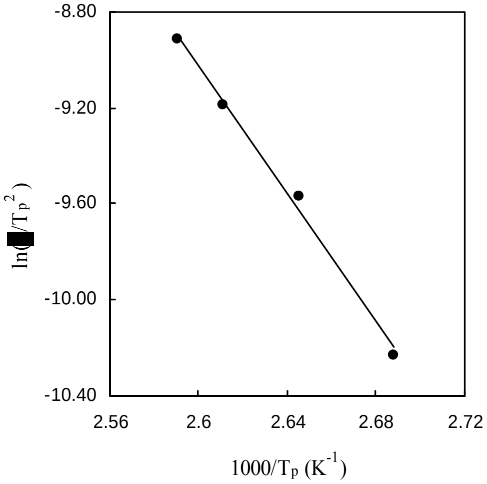

Fig. 11. A plot of $\ln(\alpha/T_p^2)$ as a function of $1000/T_p$ for $Se_{72}Sb_{20}Ag_8$

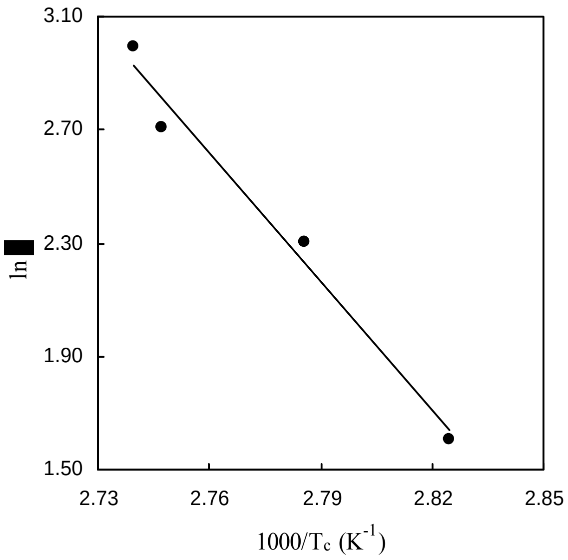

Fig. 12. A plot of ln(α) as a function of $1000/T_c$ for $Se_{72}Sb_{20}Ag_8$

In analyzing the crystallization data in DSC experiments, the Kissinger method is the most commonly used one. This equation was developed for a simple first order reaction. Kissinger showed that for first order reactions a linear dependence is obtained between α/T_p^2 and $1/T$p. It is reported [53] that Kissinger method can be applied to any reaction, the kinetics of which are described by $dx/dt=g(x)h(T)$; ($g(x)$ and $h(T)$ can be formulated since x and T are function of time). Application of this method to crystallization process without modification does not yield the same dependence as suggested by Kissinger. However, it has been suggested [54] that the error involved in the activation energy determined by Kissinger equation is lower than 5% provided $E/(RT)>10$.

To simplify the mathematical equations involved in the integration of the rate of transformation, Ozawa realized that the fraction transformed, xp, at the peak in the transformation rate, dx/dt, is constant, independently of the scan rate α. It is shown that [29] approximately 63% of the transformation occurred at the peak in dx/dt. Therefore, according to Yinnon and Uhlmann [53] if the fraction x_p at the peak of the exotherm is constant, the temperature involved in Ozawa equation is the onset crystallization temperature, T_c, or the peak temperature of crystallization T_p. This will also amplify the errors in the calculated activation energy from Eq. (10).

Matusita *et al.* [48] have suggested that the Kissinger and Ozawa equations cannot be applied directly to the crystallization of amorphous materials and therefore the physical meaning of the activation energies thus obtained are obscure because the crystallization is advanced not by the n^{th} order reaction but by the nucleation and growth process. Indeed they succeeded in obtaining an equation (Eq. 8) to analyze the non-isothermal crystallization kinetics on the basis of nucleation and growth process. This equation involved the crystallization mechanism such as bulk crystallization or surface crystallization and therefore meaningful activation energy is obtained. In this equation $n=m+1$ for as-quenched glass containing no nuclei and $n=m$ for a glass containing a sufficiently large number of nuclei. Also, m=3, 2, 1 for three, two and one-dimensional growth, respectively. They have also shown that under certain conditions, the so-called Ozawa and Kissinger equations can be deduced from Eq. (8).

The observed difference in the value of E_c evaluated by different formulations may be attributed to the different approximations that have been adopted while arriving at the final equation of the various formalism. Besides, the variability of the location of temperature measuring thermocouple (i.e. the location of sample and heat source) may introduce an error on the temperature axis of thermo analytical curve. In addition, the temperature and pressure gradients in the sample (resulting from heat effect e.g. heating rate) vary randomly and such random variations have predominant effects on kinetic parameters. Since the activation energy in the above equations has been deduced from the variation of heating rate and temperature hence variation in the value of E_c is expected to occur in the light of the reasons mentioned. However, a similar variation in the activation energy calculated by using various formalisms in other chalcogenide glasses has been observed [34, 55]. It may be mentioned that the activation energy obtained from Matusita equation is more accurate than those obtained from other methods. This is due to fact that the activation energy in this method has been derived from the variation of the temperature that scans the whole curves starting from beginning of the crystallization process till approximately its end. Besides this, it allows the determination of the dimensionality of the growth and the crystallization mechanism involved in amorphous materials.

The glass- forming tendency is calculated from Hruby's parameter [56], K_{gl}

$$K_{gl} = \frac{T_c - T_g}{T_m - T_c} \tag{11}$$

the value of K_{gl} varies from 0.28 to 0.34. A theoretical relation between T_g and T_m was given by Kauzmann [57]. It was suggested that the ratio $T_{rg} = T_g/T_m$ is constant and nearly 2/3, where T_{rg} is also called reduced glass transition temperature. This is also known as two third rule. It was found that the value of T_{rg} is same for all composition and is equal to 2/3, hence two third rule is applicable in the present study also. The value of T_c-T_g, K_{gl} and T_{rg} are listed in Table 3.

Table 3. Values of T_c-T_g, K_{gl} and T_{rg} calculated from DSC thermogram taken at 15 Kmin^{-1} heating rate for $Se_{80-x}Sb_{20}Ag_x$ ($8 \leq x \leq 14$) glassy system.

Alloy	T_g (K)	T_c (K)	T_m (K)	T_c-T_g (K)	T_m-T_c (K)	K_{gl}	T_{rg}
$Se_{72}Sb_{20}Ag_8$	326	364	492.52	37	128.52	0.29	0.662
$Se_{70}Sb_{20}Ag_{10}$	327	366	492.36	39	126.36	0.31	0.664
$Se_{68}Sb_{20}Ag_{12}$	328	369	492.36	41	123.36	0.33	0.666
$Se_{66}Sb_{20}Ag_{14}$	330	372	492.36	43	120.36	0.36	0.670

4. Conclusions

The effect of addition of Ag to the Se-Sb system on the crystallization kinetics and thermal stability of the material has been investigated. It is found that the glass transition temperature and the crystallization temperature increase with increase in Ag content to the Se-Sb system as well as with increase in heating rate. It has been found that the value of crystallization temperature is much higher than the room temperature, which gives an important advantage that is essential to prevent self-transition of recording materials between the two phases amorphous and crystalline phase at room temperature. The apparent activation energies of glass transition and the crystallization have been determined and found to be close for most of the theoretical approaches. All the samples follow the well-known two third rule.

Acknowledgements

The authors thank CIL/SAIF Punjab University, Chandigarh for their valuable help in taking XRD and NIPER, Mohali for their help in getting DSC scans.

References

[1] D. P. Gosain, T. Shimizu, M. Ohmuru, M. Suzuki, T. Bando, S. Okano, J. Mat. Sci. **26**, 3271 (1991).
[2] N. Nobukuni, M. Takashima, T. Ohno, M. Horie, J. Appl. Phys. **78**, 6980 (1995).
[3] L. Men, F. Jiang, F. Gan, Mater. Sci. Eng. B **47**, 18 (1997).
[4] A. K. Kolobov, J. Tominaga, J. Optoelectron. Adv. Mater. **4**, 679 (2002).
[5] S. A. Khan, M. Zulfequar, M. Husain, Vacuum **72**, 291 (2003).
[6] N. Mehta, M. Zulfequar, A. Kumar, J. Optoelectron. Adv. Mater. **6**, 441 (2004).
[7] P. Pradeep, N. S. Saxena, A. Kumar, J. Phys. Chem. Solids **3**, 385 (1997).
[8] R. A. Ligero, J. V. Azquez, M. Lucas-Ruiz, R. Jimenez Garay, Thermochem. Acta **197**, 319 (1992).
[9] K. Tanaka, Phys. Rev. B **39**, 270 (1989).
[10] K. Tanaka, J. Non-Cryst. Solids **164-166**, 1179 (1993).
[11] T. Wagner, R. Jilkova, M. Frumar, M. Vicek, Int. J. Electron. **77**, 185 (1994).
[12] K. Tanaka, M. Itoh, N. Yoshida, M. Ohto, J. Appl. Phys. **78**, 3895 (1995).
[13] T. Kawaguchi, S. Maruno, S. R. Elliott, J. Appl. Phys. **79**, 9096 (1996).
[14] M. Ohto, Phys. Status Solidi a **159**, 461 (1997).
[15] T. Wagner, M. Frumar, V. Suskova, J. Non-Cryst. Solids **128**, 197 (1991).
[16] M. Frumar, Z. Polak, Z. Cernosek, B. Frumarova, T. Wagner, Chem. Papers **57**, 310 (1997).
[17] T. Wagner, J. Optoelectron. Adv. Mater. **4**, 717 (2002).
[18] K. Ramesh, S. Asokan, K. S. Sangunni, E. S. R. Gopal, J. Phys. Chem. Solids **61**, 95 (2000).
[19] G. F. Zhou, Mater. Sci. Eng. A **73**, 304 (2001).
[20] J. Gutwirth, T. Wagner, T. Kohoutek, Mir Vlcek, S. Schroeter, V. Kovanda, Mil Vlcek, M. Frumar, J. Optoelectron. Adv. Mater. 5, 1139 (2003).
[21] L. H. Chou, Y. Y. Chang, Y. C. Chai, S. Y. Wang, J. Appl. Phys. Part 1 **40**, 4924 (2001).
[22] D. Sharma, R. K. Shukla, A. Kumar, Thin Solid Films **357**, 214 (1999).
[23] M. F. Kotkata, C. S. Mohamed, M. M. Radwan, J. Mater. Sci. **25**, 482 (1990).
[24] M. Kitao, C. Gotoh, S. J. Yamada, J. Mater. Sci. **30**, 3521 (1995).
[25] D. Sharma, R. K. Shukla, A. Singh, A. K. Nagpal, A. Kumar, Adv. Mater. Opt. Electron. **10**, 251 (2000).
[26] M. Lasoka, Mat. Sci. Eng. **23**, 173 (1976).
[27] S. R. Joshi, A. Pratap, N. S. Saxena, M. P. Saksena, A. Kumar, J. Mat. Sci. Lett. **13**, 77 (1994).
[28] H. E. Kissinger, J. Res. Nat. Bur. Stand. **57**, 331 (1956).
[29] H. S. Chen, J. Non-Cryst. Solids **27**, 257 (1978).
[30] J. A. Macmillan, J. Phys. Chem. **42**, 3497 (1965).
[31] J. Colemenero, J. M. Barandiaran, J. Non-Cryst. Solids **30**, 263 (1978).
[32] J. E. Shelby, J. Non-Cryst. Solids **34**, 111 (1979).
[33] M. M. A. Imran, D. Bhandari, N. S. Saxena, Physica B **293**, 394 (2001).
[34] S. Mahadevan, A. Giridhar, A. K. Singh, J. Non-Cryst. Solids **88**, 11 (1986).
[35] W. A. Johnson, K. F. Mehl Trans. Amer. Inst. Mining Met. Egrs. **135**, 315 (1981).
[36] M. Avrami. J. Chem. Phys. **7**, 1103 (1939).
[37] M. Avrami, J. Chem. Phys. **8**, 212 (1940).
[38] M. Avrami, J. Chem. Phys. **9**, 177 (1941).
[39] M. M. El-Zaidia, A. El-Shafi, A. A. Ammar, M. Abo-Ghazala, J. Mat. Sci. **22**, 1618 (1987).
[40] P. Pradeep, N. S. Saxena, M. P. Saksena, A. Kumar, Physica Scripta **54**, 207 (1996).
[41] D. W. Henderson, J. Non-Cryst. Solids **30**, 301 (1979).
[42] M. M. A. Imran, D. Bhandari, N. S. Saxena, Physica Scripta **61**, 502 (2000).
[43] J. W. Cahn, Acta. Metal. **4**, 572 (1956).
[44] G. S. Melling, D. R. Uhlmann, Phys. Chem. Glasses **2**, 62 (1967).
[45] N. Raysava, L. Tichy, C. Barta, A. Triska, H. Ticha, Phys. Stat. Sol. **87**, 13 (1985).
[46] V. R. V. Ramanan, G. E. Fish, J. Appl. Phys. **53**, 2273 (1982).
[47] K. White, R. L. Crane, J. Non-Cryst. Solids **103**, 210 (1988).

[48] K. Matusita, T. Komatsu, R. Yokota, J. Mat. Sci. 19, 291 (1984).
[49] J. Colemenero, J. M. Barrandiran, J. Non-Cryst. Solids **21**, 411 (1976).
[50] P. Dhuaj, B. Baranock, A. Ondrejka, J. Non-Cryst. Solids **18**, 210 (1986).
[51] R. F. Speyer, S. H. Risbud, Phys. Chem. Glasses **24**, 26 (1983).
[52] T. Ozawa, Polymer **12**, 150 (1971).
[53] H. Yinnon, D. R. Uhlmann, J. Non-Cryst. Solids **54**, 253 (1983).
[54] J. M. Criado, A. Ortega, J. Non-Cryst. Solids **87**, 302 (1986).
[55] A. B. Abd El-Moiz, N. Afify, M. M. Hafiz, Physica B **18**, 33 (1992).
[56] Hruby, Czech, J. Phys. B **22**, 1187 (1992).
[57] W. Kauzmann, Chem. Rev. **43**, 219 (1948).